Structural Engineering and Mechanics, Vol. 7, No. 4 (1999) 377-386
DOI: http://dx.doi.org/10.12989/sem.1999.7.4.377

Stress analysis of a postbuckled laminated composite plate

Gin-Boay Chai† and Siaw Meng Chou†

School of Mechanical and Production Engineering, Nanyang Technological University, Nanyang Avenue, Singapore 639798

Chee-Leong Ho‡

Ministry of Defence, Singapore

Abstract. The stress distribution in a symmetrically laminated composite plate subjected to in-plane compression are evaluated using finite element analysis. Six different finite element models are created for the study of stresses in the plate after buckling. Two finite element modelling approaches are adopted to obtain the stress distribution. The first approach starts with a full model of shell elements from which sub-models of solid elements are spin-off. The second approach adopts a full model of solid elements at the beginning from which sub-models of solid elements are created. All sub-models have either 1-element thickness or 14-element thickness. Both techniques show high interlaminar direct and shear stresses at the free edges. The study also provides vital information of the distribution of all components of stresses along the unloaded edges in length direction and also in the thickness direction of the plate.

Key words: laminate; composite plate; buckling; stability; stress analysis; interlaminar shear

1. Introduction

Modern technologies demand materials with unusual combinations of properties that cannot be provided by most conventional metals, alloys, ceramics, and polymeric materials. Aerospace, underwater and transportation application are typical examples where there are strong demand for material properties which exhibit a good combination of low density, high strength, good impact and abrasion resistance and inert to environmental condition. However, most materials do not have strength and toughness at the same time. Furthermore, high strength and low density materials are usually expensive. Most metals require special treatment to prevent oxidization. On the other hand, composite materials offer the above advantages by combining different form of materials.

There are numerous research papers written on the study of the buckling (Jones 1975, Whitney 1987, Leissa 1981, Chai and Khong 1991 *et al.*) and postbuckling behaviour of composite plate

† Senior Lecturer
‡ Mechanical Engineer

(Yusuff 1952, Chia 1972, Harris 1973, Banks and Harvey 1977 *et al.*). Very few research papers however emphasized the stress distribution and failure aspect of the postbuckled composite plate. Davies, Buskell and Steven (1985) investigated the failure of carbon fibre composite panel subjected to compression. They postulated that failure was precipitated by interlaminar shear stresses near the edge due to both membrane forces and twisting moment. The presence of these stresses reduced the strength of the panel up to 40%. They confirmed that the source for the delamination was due to shear, rather than tensile peeling. Chai and Hoon (1994) and Chai *et al.* (1996) analysed large deflection and failure of symmetrically laminated composite plates under compression using finite element method. Their analysis did not include a thorough inspection of the stress distribution and the possible modes of failure in the postbuckled plate. Their results showed that the predicted failure load using the Tsai-Wu failure criterion (and first-ply failure only) agreed to a reasonable degree with experimental results.

The use of analytical approaches in analysing composite structural behaviour is very good in conducting extensive parametric studies of structural instability. But its general use is rather more limited in scope than the versatile finite element method. Nowadays finite element computer codes are easily available and affordable. The purpose of this paper is to exploit the use of existing finite element computer codes to analyse the 3-dimensional stresses in a postbuckled laminated composite plate. In a way the paper also serves as an aid in understanding the critical stresses set up in a laminated composite plate subjected to in-plane load beyond buckling.

2. Finite element models

The commercially available finite element computer source code ANSYS (1994) is used in the investigation. The plate model is a 458 mm by 90 mm composite plate which comprised of 14 layers of unidirectional Grafil XAS fibres impregnated in Fibredux 914C epoxy resin. Each layer is 0.125 mm thick and total panel thickness is 1.75 mm. The material properties of the unidirectional laminae used in the analysis is E_{11}=130GPa, E_{22}=9GPa, G_{12}=4.8GPa and ν_{12}=0.28. The loaded ends are clamped while the long unloaded edges are simply supported. Incremental uniform displacement is applied at one of the loaded ends while the opposite end is fully constrained. Fig. 1 shows the coordinate system and the constraints applied along the edges of the

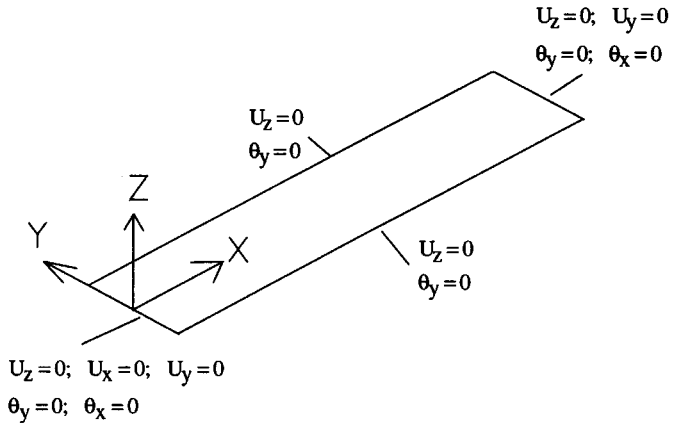

Fig. 1 Coordinate system and boundary conditions of the model

finite element model.

In finite element method of analysis, there are usually two options to obtain an accurate result in regions where there are geometrical discontinuities (stress concentrations) or where stress gradients are high such as interlaminar stresses at the edge of a laminate: 1) reanalyse the entire model with greater mesh refinement, or 2) use sub-modelling technique to generate an independent, more finely meshed model of only the region of interest and analyse it. The first option can be time-consuming and may not be economical. The sub-modelling technique is used in this paper. The technique is also known as the cut-boundary displacement method. The cut boundary is the boundary of the sub-model which represents a cut through the coarse model. Displacements calculated on the cut boundary of the coarse model are specified as boundary conditions for the sub-model.

Two approaches will be used, the first uses shell elements for its full model while the second uses solid elements for its full model. Hence two of the six models are full size plate models, namely 458 mm by 90 mm with a thickness of 1.75 mm. The others are the sub-models (about 229 mm by 45 mm) of the two full size models. The models are each given a name as described in Table 1. The mesh density of the models are also indicated in the table, for 8×30 model refers to 8 elements across the width of the plate and 30 elements along the length of the plate.

Two types of elements are utilized for the modelling; 8-node layered structural solid element and 8-node layered structural shell element. Both element types are specially designed to model composite material effectively. The shell element has both bending and membrane capabilities, and has 6 degree-of-freedom at each node (3 translations and 3 rotations). The solid element has only 3 translational degree-of-freedom at each node but it has three dimensional stress analysis capability.

The calculation of interlaminar shear stress in the shell element is based on the assumption that there are no interlaminar shear stresses at the outer surface of the shell. This assumption cannot be used in the formulation of the solid element. Calculation of the interlaminar shear stress in the element is either based on the nodal forces or based on the strain-displacement relationship. Neither of these is exact, but on the whole they will agree with each other. Additional elements in the thickness direction usually improve the interlaminar shear stress calculation. Since the solid element is a lower order element, finer meshes may be required for shell applications to provide the same accuracy as the shell element.

Table 1 Description for the six models

No	Model Name	Description
1	P	8×30 Shell model
2	S	12×60 Solid model
3	P1	10×60 Sub-model from model P using shell-to-solid sub-modelling. 1-element thickness
4	S1	10×60 Sub-model from model S using solid-to-solid sub-modelling. 1-element thickness
5	P14	5×40 Sub-model from model P using shell-to-solid sub-modelling. 14-element thickness
6	S14	5×40 Sub-model from model S using solid-to-solid sub-modelling. 14-element thickness

Table 2 Buckling load for the various models

No	Model	Buckling load	End shortening at buckling (mm)
1	8×30 Shell	9.062	0.3114
2	8×40 Shell	9.072	0.3118
3	Large deflection theory (Chai 1991)	9.748	0.3357
4	12×60 Solid	9.203	0.3157
5	20×100 Solid	9.074	0.3113
6	Linear buckling theory (Chai and Hoon 1992)	9.194	0.3166
7	Finite strip method (Chai and Khong 1991)	10.332	0.3558

3. Numerical results

Prior to performing a non-linear analysis of the plate model and its sub-model, a preliminary linear buckling analysis is carried out. The buckling results are shown in Table 2 for two shell models and two solid models. In addition Table 2 also gives theoretical results obtained from 3 different published sources (Chai and Khong 1991, Chai and Hoon 1992, Chai 1991). The large deflection theory by Chai (1991) is formulated for simply supported laminated composite plates. It is used here as a basis for comparison since for long plates the boundary conditions along the loaded ends have negligible effect on the buckling result of the plate (Chai and Hoon 1992).

The linear buckling theory by Chai and Hoon (1992) used a 144-term trigonometric deflection function in the energy formulation to include the effect of the bending/twisting coupling and can be termed as the "accurate" solution. The finite strip method by Chai and Khong (1991) is less accurate since this coupling term was ignored in the formulation. As it can be seen from Table 2 that the percentage difference between the 2 solid models is only 1.42% and they agreed very well with the linear buckling results (Chai and Hoon 1992). It can also be observed that the

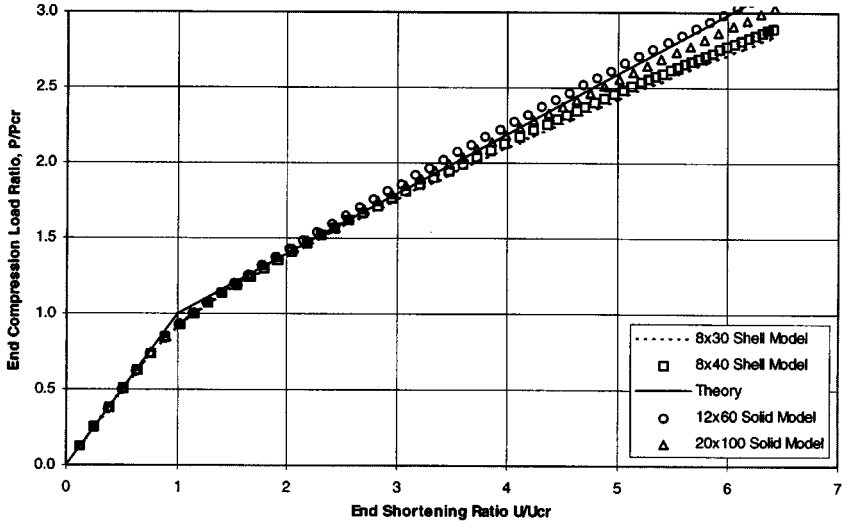

Fig. 2 Comparing the load-end shortening curves of the various models

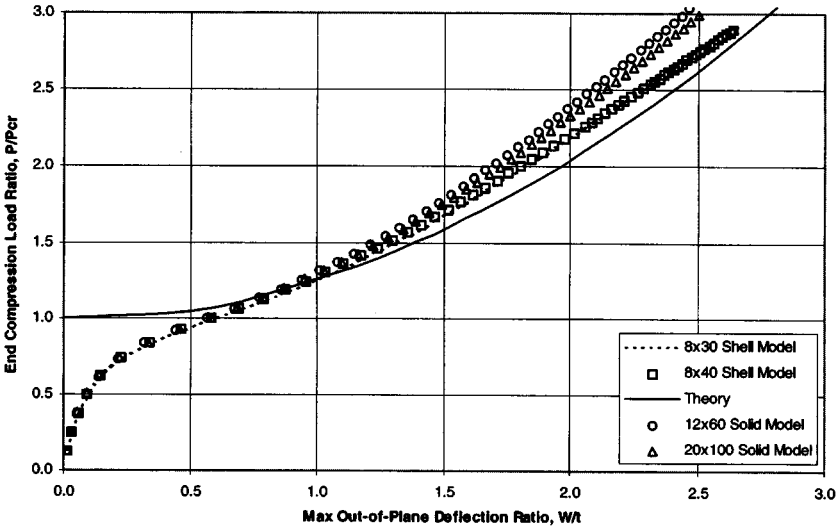

Fig. 3 Comparing the load-max deflection curves of the various models

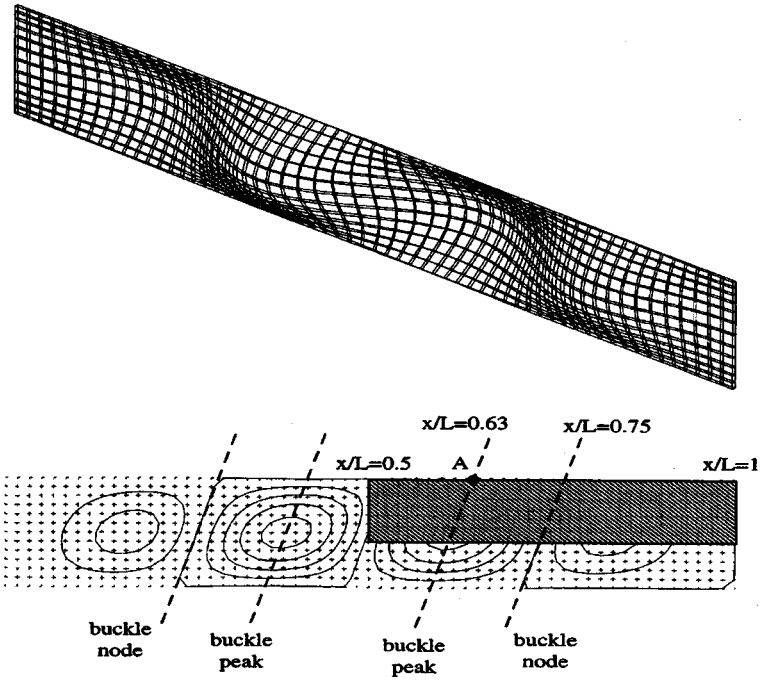

Fig. 4 An illustration of the submodel region (shaded)

results of the solid element models require much finer mesh density to achieve those of the shell element models.

The non-linear analysis of these finite element models is next carried out based on a 10% initial geometrical imperfection of the plate. The comparison of these results are shown in Fig. 2 for the load-end shortening response and Fig. 3 for the load-maximum out-of-plane deflection response.

Included in the figures is also the result of the large deflection theory of Chai (1991). The comparison shows that the results of the finite element models follow closely those of the theoretical prediction.

From the results presented in Figs. 2, 3 and Table 2, it is decided to use the 8×30 Shell and 12×60 Solid models for the subsequent sub-modelling analysis. As explained earlier sub-

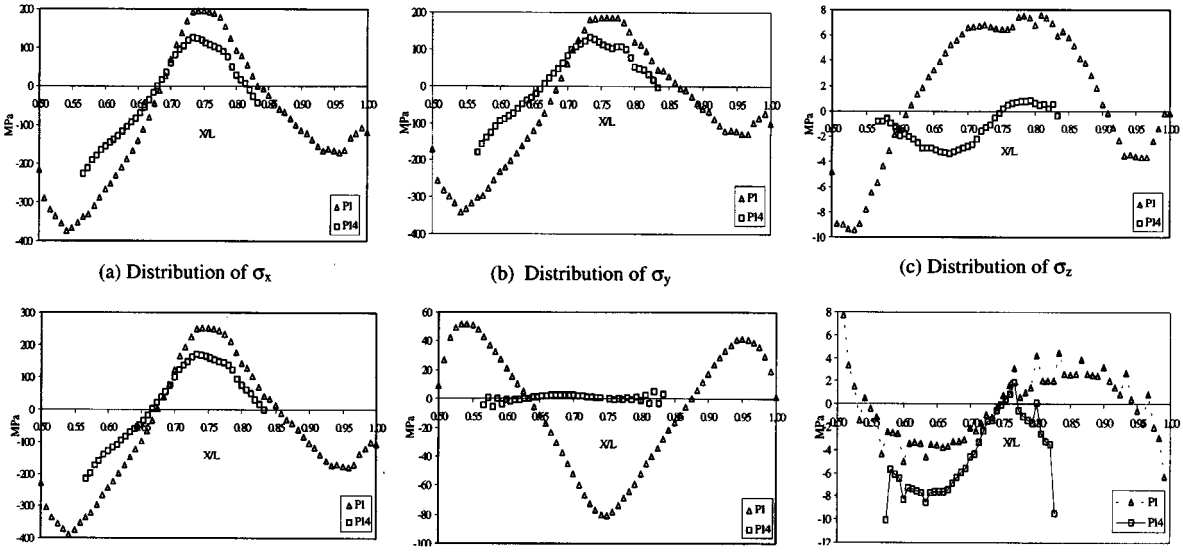

(a) Distribution of σ_x (b) Distribution of σ_y (c) Distribution of σ_z

(d) Distribution of τ_{xy} (e) Distribution of τ_{xz} (f) Distribution of τ_{yz}

Fig. 5 Stress distribution in the length direction

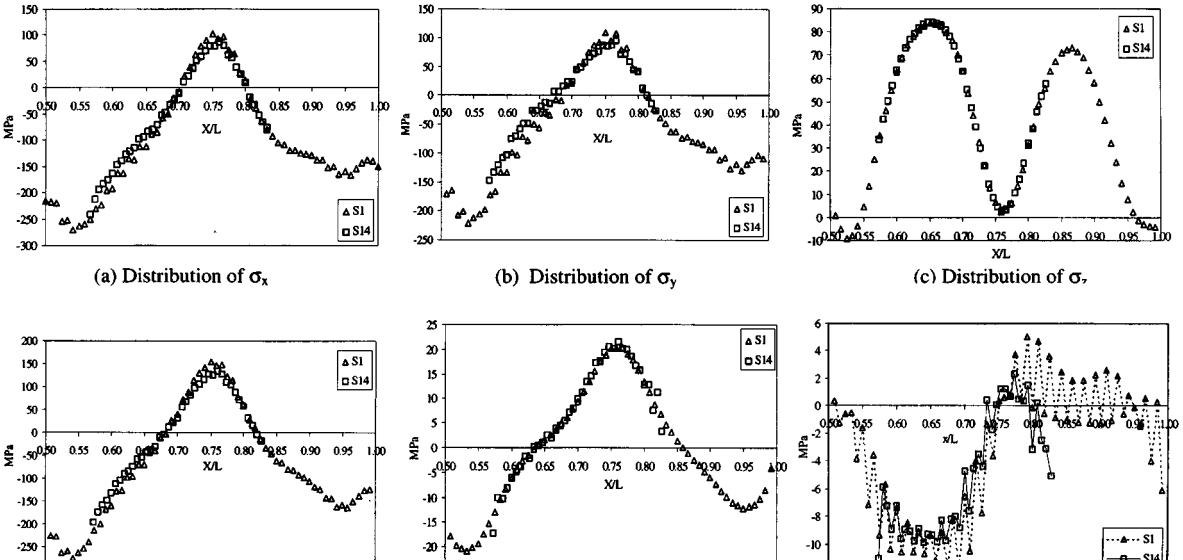

(a) Distribution of σ_x (b) Distribution of σ_y (c) Distribution of σ_z

(d) Distribution of τ_{xy} (e) Distribution of τ_{xz} (f) Distribution of τ_{yz}

Fig. 6 Stress distribution along the length

modelling is required as the accurate prediction of the three dimensional stresses, in particular the interlaminar shear stresses, near the unloaded edge of the plate depend very much on the fine mesh density used in the modelling. The sub-model region used for the detailed investigation is illustrated in Fig. 4, which also shows the buckled mode shape of plate. The description of each of the models are explained in Table 1.

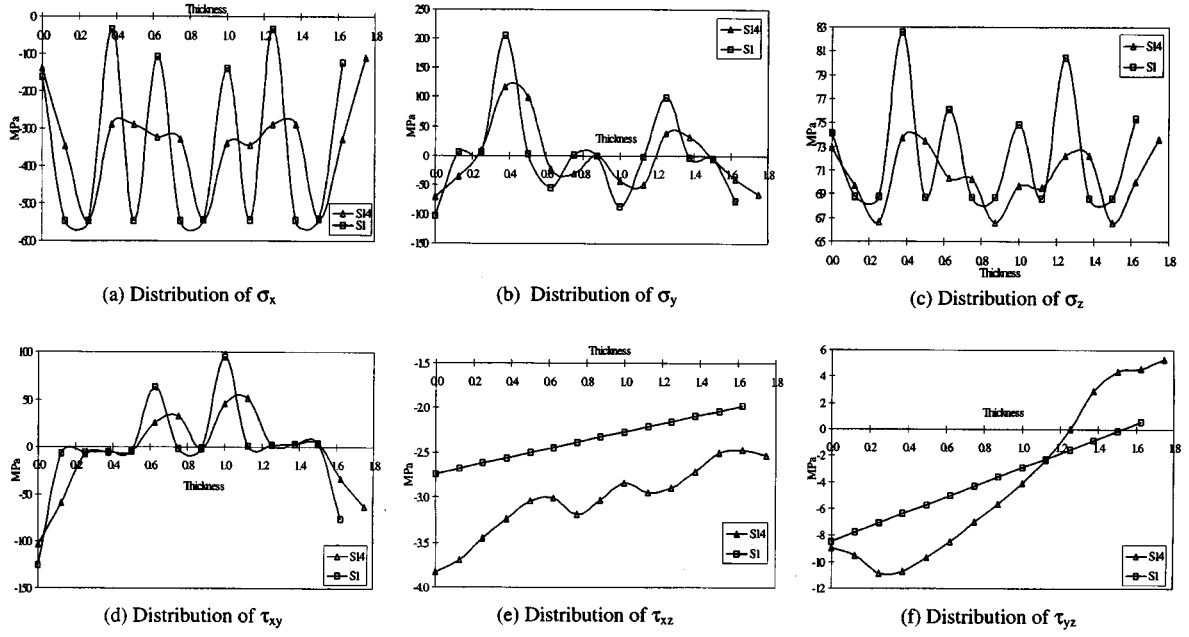

(a) Distribution of σ_x (b) Distribution of σ_y (c) Distribution of σ_z

(d) Distribution of τ_{xy} (e) Distribution of τ_{xz} (f) Distribution of τ_{yz}

Fig. 7 Stress distribution through thickness

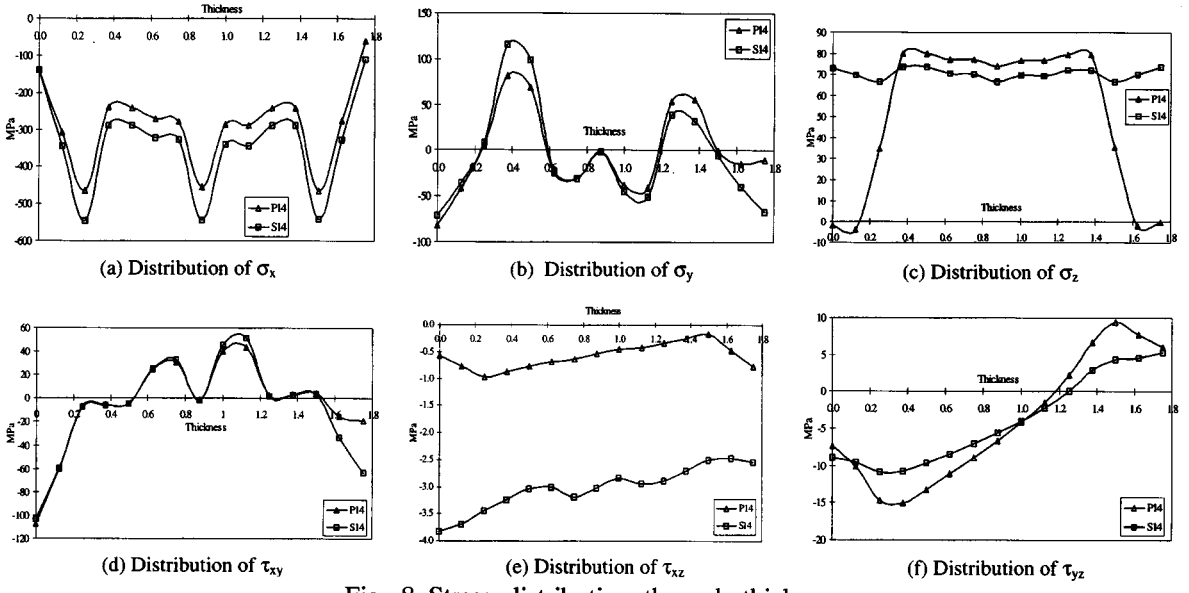

(a) Distribution of σ_x (b) Distribution of σ_y (c) Distribution of σ_z

(d) Distribution of τ_{xy} (e) Distribution of τ_{xz} (f) Distribution of τ_{yz}

Fig. 8 Stress distribution through thickness

The stress distribution shown in Figs. 5 to 8 are stresses obtained from the various finite element sub-models at an applied end shortening of 1.4 mm (about 4.5 times the end shortening at buckling). The stresses for the sub-models P1 and P14 are presented together to study the effect of finer mesh in the thickness direction. Figs. 5(a) to 5(f) show the distribution of stresses σ_x, σ_y, σ_z, τ_{xy}, τ_{xz} and τ_{yz} respectively at the edge of the plate and along the top surface of the plate for sub-models P1 and P14. Figs. 5(a), 5(b), 5(d) and 5(f) show that the trend of σ_x, σ_y, τ_{xy} and τ_{yz} is similar but show significant difference in magnitudes. In Figs 5(c) and 5(e), sub-models P1 and P14 show completely different trend and magnitudes of σ_z and τ_{xz}. In general, the stress distribution on the surfaces of the solid models are affected by the number of elements in the thickness direction. In particular the prediction of the distribution of σ_z and τ_{xz} are completely different and can be a crucial factor when deciding the failure modes of the plate.

Similarly the comparison of the stress distribution between the sub-models S1 and S14 along the unloaded edge is shown in Fig. 6. It can be seen that the stress distribution throughout is in good agreement, meaning finer meshing in the thickness direction did not affect the results. The major difference between the sub-models P1-P14 and S1-S14 is in the distribution of the stress components σ_z and τ_{xz}. The sub-models S1 and S14 show a maximum σ_z of 85 MPa at x/L=0.65 as shown in Fig. 6(c) and a maximum τ_{xz} of 23 MPa at x/L=0.75 as shown in Fig. 6(e). However the sub-models P1 and P14 show an entirely different distribution and magnitudes of σ_z and τ_{xz} as shown in Figs. 5(c) and 5(e).

A point at the unloaded edge near the buckle peak line (point A in Fig. 4, x/L=0.63) is selected for detailed study of the stress distribution in the thickness direction. The stress results for sub-models S1 and S14 are shown in Fig. 7 and for sub-models P14 and S14 in Fig. 8. In Fig. 7, it is obvious that the peak stresses depend on the number of element in the thickness direction. In Fig. 8, comparing the results of two sub-models P14 and S14 show significant difference in the prediction of the stress distribution. Model P14 has a near zero value of σ_z at the external surfaces (this is to be expected) but reached to a similar magnitude as model S14 in most portion of the thickness as shown in Fig. 8(c). Another major difference is that τ_{xz} in model S14 has a much higher value through the thickness, as shown in Fig. 8(e).

It has been envisaged that the difference in the stresses between the shell and the solid models could be a result of ill conditioning, shear locking and instability of the element stiffness matrix during the computation of the finite element model. Either as a result of the large side-to-thickness ratio in thin plates where transverse shear strains become negligible or as a result of poor choice of quadrature rule, the element stiffness matrix becomes stiff and hence these problems arise and yield erroneous results (Reddy 1985, Cook and Malkus 1989). This was however ruled out because of the extensive error checking tests written in the computer programme code, and also because of the numerous extensive validations of the finite element results with the results obtained from theoretical calculations and from experiments (Chai and Hoon 1994 and Chai *et al.* 1996).

4. Conclusions

The two full finite element models of the laminated composite plate using shell and solid elements are verified both at buckling and beyond buckling. Four sub-models are derived from the two full plate models to investigate further the three dimensional stresses in the plate. The results from the sub-models show high value of interlaminar stress occurring at the unloaded edges.

Using more solid elements in the thickness direction, it was found that the interlaminar shear stress vary considerably over the thickness.

Two main conclusions can be drawn from the numerical study:

1) The submodels from the full shell model (models P1 and P14) are sufficient as they save time and computational costs, if interlaminar shear stresses are not required in the analysis.
2) If detailed analysis of the 3-D stresses are required, then the submodels from the full solid model (models S1 and S14) would be the best. They maybe more costly and take longer computational time but they give a more detailed and "accurate" distribution of all the stresses.

The sub-model S14 gave high value of σ_z at the unloaded edges near the buckle peak line and also show a high value of τ_{xz} at the unloaded edge around the buckle node line. Due to the low modulus and strength of the interply adhesive layer, these two stresses could influence the failure modes of the laminated composite plate subjected to load beyond buckling. The next step of this work is to investigate into the contribution of each of these stresses towards the initial and final failure of the laminated composite plate.

References

ANSYS Engineering Analysis System Theoretical Manual, Revision 5.0 (1994), Swanson Analysis Systems Inc., Pennsylvania, U.S.A.

Baharlou, B. and Leissa, A.W. (1987), "Vibration and buckling of generally laminated composite plates with arbitrary edge conditions", *Int. J. Mech. Sci.*, **29**(9), 545-555.

Banks, W.M. and Harvey, J.M. (1977), "Large deflection of orthotropic plates", *Acta Technica Academiae Scientiarum Hungaricae*, Tomus 87 (1-2), 21-36.

Buckling and Postbuckling of Composite Plates (1975), edited by G.J. Turvey and I.H. Marshall, Chapman & Hall, London.

Buskell, N., Davies, G.A.O. and Stevens, K.A. (1985), "Postbuckling failure of composite panels", *Proceedings of the Third International Conference on Composite Structures*, Elsevier Applied Science, England, 677-91.

Chai, G.B. (1991), "Large deflection of laminated composite plates", *Composite Science and Technology*, **42**(4), Elsevier Science Publishers, England, 349-360.

Chai, G.B., Banks, W.M. and Rhodes, J. (1991), "The instability behaviour of laminated panels with elastically rotationally restrained edges", *Composite Structures* **19**(1), Elsevier Science Publishers, England, 41-65.

Chai, G.B., Banks, W.M. and Rhodes, J. (1991), "An experimental study on laminated panels in compression", *Composite Structures* **19**(1), Elsevier Science Publishers, England, 67-87.

Chai, G.B. and Hoon, K.H. (1994), "Numerical and experimental study of large deflection of symmetrically laminated composite plates in compression", *Structural Engineering and Mechanics, An Int. J.* **2**(4), 359-367.

Chai, G.B., Hoon, K.H., Chin, S.S. and Soh, A.K. (1996), "Stability and failure of symmetrically laminated plates", *Structural Engineering and Mechanics, An Int. J.* **4**(5), 485-496.

Chai, G.B. and Hoon, K.H. (1992), "Buckling of generally laminated composite plates", *Composites Science and Technology*, **45**, 125-133.

Chai, G.B. and Khong, P.W. (1991), "Stability study of coupling responses in laminates", *Journal of Composites Technology & Research*, **13**(3).

Chia, C.Y. (1972), "Large deflection of rectangular orthotropic plates", *Trans ASME Jnl Engrg Mech*, 1285-1297.

Harris, G.Z. (1973), "Instability of laminated composite plates", *AGARD Conf Proc.* 112, 14.

Iyengar, N.G.R. (1988), *Structural Stability of Columns and Plates*, Ellis Horwood.
Jones, R.M. (1975), *Mechanics of Composite Materials*, Hemisphere, New York.
Kapania, R.K. and Raciti, S. (1989), "Recent advances in analysis of laminated beams and plates, Part I: shear effects and buckling", *AIAA Journal*, **27**(7), 923-934.
Leissa, A.W. (1981), "Advances in vibration, buckling and postbuckling studies on composite plates", *Composite Structures*, Ed by I H Marshall, London, Applied Science Publishers Ltd., 312-334.
Leissa, A.W. (1983), "Buckling of composite plates", *Composite Structures*, **1**, 51-66.
Leissa, A.W. (1987), "An overview of composite plate buckling", *Composite Structures*, **4**(1), 1-29.
Stein, M. (1983), "Postbuckling of orthotropic composite plates loaded in compression", *AIAA Jnl* **11**(12), 1729-1735.
Whitney, J.M. (1987), *Structural Analysis of Laminated Anisotropic Plates*, Technomic, Lancaster, USA.
Yusuff, S. (1952), "Large deflection theory for orthotropic rectangular plates subjected to edge compression", *J. Appl Mech* **19**, 446-450.

Notations

L	: Length of plate.
x/L	: Ratio of distance along the x axis to plate's length.
W/t	: Ratio of maximum out-of-plane deflection to plate's thickness.
x, y, z	: Rectangular coordinates.
$\sigma_x, \sigma_y, \sigma_z$	: Direct stress in x, y and z respective direction.
$\tau_{xy}, \tau_{xz}, \tau_{yz}$	: Shear stress in x-y, x-z and y-z respective plane.